doi:10.1111/evo.12390

GENETIC ARCHITECTURE OF SKELETAL EVOLUTION IN EUROPEAN LAKE AND STREAM STICKLEBACK

Daniel Berner,[1,2] Dario Moser,[1] Marius Roesti,[1] Heinz Buescher,[1] and Walter Salzburger[1]

[1]*Zoological Institute, University of Basel, Vesalgasse, 1, CH-4051 Basel, Switzerland*

[2]*E-mail: daniel.berner@unibas.ch*

Received October 4, 2013
Accepted February 11, 2014

Advances in genomic techniques are greatly facilitating the study of molecular signatures of selection in diverging natural populations. Connecting these signatures to phenotypes under selection remains challenging, but benefits from dissections of the genetic architecture of adaptive divergence. We here perform quantitative trait locus (QTL) mapping using 488 F_2 individuals and 2011 single nucleotide polymorphisms (SNPs) to explore the genetic architecture of skeletal divergence in a lake-stream stickleback system from Central Europe. We find QTLs for gill raker, snout, and head length, vertebral number, and the extent of lateral plating (plate number and height). Although two large-effect loci emerge, QTL effect sizes are generally small. Examining the neighborhood of the QTL-linked SNPs identifies several genes involved in bone formation, which emerge as strong candidate genes for skeletal evolution. Finally, we use SNP data from the natural source populations to demonstrate that some SNPs linked to QTLs in our cross also exhibit striking allele frequency differences in the wild, suggesting a causal role of these QTLs in adaptive population divergence. Our study paves the way for comparative analyses across other (lake-stream) stickleback populations, and for functional investigations of the candidate genes.

KEY WORDS: **Effect size, *Gasterosteus aculeatus*, lateral plate, QTL mapping, RAD sequencing, vertebral number.**

Exploring the genetic basis of adaptation promises to illuminate several long-standing issues in biological diversification. These include the number and genomic location of genetic changes underlying adaptation, their role in developmental pathways, their phenotypic effects and resulting ecological consequences, and their predictability (Orr 1998; Barton and Keightley 2002; Phillips 2005; Hoekstra and Coyne 2007; Mitchell-Olds et al. 2007; Wray 2007; Arendt and Reznick 2008; Stern and Orgogozo 2008; Mackay et al. 2009; Rockman 2011; Wake et al. 2011; Yeaman and Whitlock 2011). Currently, perhaps the most popular approach to investigating the genetics of adaptation is divergence mapping (Nielsen 2005; Storz 2005; Oleksyk et al. 2010). Here a large set of genome-wide molecular markers is screened for putative signatures of divergent selection between ecologically distinct populations. In well-developed empirical systems, this is proving a powerful method for the discovery of genomic regions or candidate genes involved in adaptive divergence (e.g., Akey et al. 2002; Voight et al. 2006; Hohenlohe et al. 2010; Lawniczak et al. 2010; Jones et al. 2012; Nadeau et al. 2012; Roesti et al. 2012a, 2014; Mateus et al. 2013; Stölting et al. 2013). A shortcoming of divergence mapping, however, is that in general molecular signatures alone cannot tell us much about the traits actually targeted by selection (Mitchell-Olds et al. 2007; Stinchcombe and Hoekstra 2008; Storz and Wheat 2010). In the years to come, we can thus anticipate a surge of information about genome regions putatively influenced by divergent selection in many organisms, but knowledge about the phenotypes transferring selection to the molecules is likely to lag behind. Understanding the genetics of adaptation will thus benefit greatly from the combination of purely genomic investigations with extensive data on the genetic architecture of phenotypic divergence, as for instance obtained by quantitative trait locus (QTL) mapping.

In the present study, we report a QTL mapping experiment performed in a powerful system for studying adaptive divergence:

EVOLUTION
INTERNATIONAL JOURNAL OF ORGANIC EVOLUTION

lake and stream populations of threespine stickleback fish (*Gasterosteus aculeatus*). Following the retreat of the last Pleistocene ice sheets, the colonization of freshwater by ancestral marine stickleback has resulted in the establishment of numerous populations occurring in adjacent lake and stream habitats (Reimchen et al. 1985; Lavin and McPhail 1993; Thompson et al. 1997; Hendry and Taylor 2004; Berner et al. 2008, 2010a; Aguirre 2009; Bolnick et al. 2009; Deagle et al. 2012; Moser et al. 2012; Lucek et al. 2013; Ravinet et al. 2013). Lake and stream stickleback are often ecologically divergent, with the most consistent difference concerning their foraging modes: lake stickleback partly or exclusively exploit pelagic food resources (zooplankton), whereas stream stickleback generally use benthic prey (macroinvertebrates; Gross and Anderson 1984; Berner et al. 2009; Kaeuffer et al. 2012; Moser et al. 2012; Ravinet et al. 2013). This divergence in foraging modes is associated with relatively consistent phenotypic differences in traits presumably important for prey capture and handling, such as overall body shape and gill raker structure (Reimchen et al. 1985; Lavin and McPhail 1993; Berner et al. 2008, 2009, 2010a; Kaeuffer et al. 2012; Lucek et al. 2013; Ravinet et al. 2013). The existence of replicate, ecologically and phenotypically divergent population pairings makes lake-stream stickleback an appealing system for the search of molecular signatures of divergent selection. Indeed, divergence mapping has already been performed in some lake-stream stickleback systems (Deagle et al. 2012; Roesti et al. 2012a).

By contrast, very little is known about the genetics of phenotypic divergence between lake and stream stickleback. Quantitative genetic (common-garden) experiments have demonstrated a genetic basis to divergence in some foraging traits (Lavin and McPhail 1993; Sharpe et al. 2008; Berner et al. 2011), but QTL dissections of the genetic architecture of phenotypic divergence have yet to be performed. We here take up this challenge by using QTL mapping to explore the genetic basis of divergence in skeletal features between lake and stream stickleback populations from Central Europe.

Materials and Methods

CROSS

Our study is based on an F_2 intercross population derived from a single *in vitro* cross of a male from Lake Constance (sampled at the ROM lake site described in Berner et al. 2010a) with a female from a stream draining into Lake Geneva (the CHE stream site in Berner et al. 2010a). The F_2 panel comprises 492 individuals (251 males, 237 females) selected haphazardly at one year of age from 35 separate F_1 crosses, each produced by a unique full-sib pairing. All details on crossing, husbandry, and handling are exactly as described in Roesti et al. (2013), a recombination study based on a subset of 282 individuals from the full F_2 population used here for QTL mapping.

All fish were euthanized with an overdose of MS-222, photographed immediately as described in Berner et al. (2009), and stored in absolute EtOH. After six months of preservation, a fin clip was taken for genetic analysis and each individual was subjected to a digital X-ray scan of the whole body and a higher resolution scan of the head. This was performed by using a Faxitron Digital Specimen Radiography System LX-60 (tube voltage 35 kV, tube current 0.3 mA), including a reference size scale in all scans.

PHENOTYPING

Our study focuses on aspects of skeletal morphology, here defined broadly as bone traits. The first trait of interest was the length of the gill rakers (bony tubercles) located on the first branchial arch (Fig. 1). Gill rakers are important to foraging because they influence prey retention and handling performance (Gerking 1994; Sanderson et al. 2001). In particular, longer gill rakers generally promote foraging on small prey items (such as zooplankton), whereas shorter gill rakers are favored in fish foraging on larger prey (such as macroinvertebrates). Indeed, the natural source populations of our cross are highly divergent in this trait, with the lake population displaying 25% longer size-corrected gill rakers than the stream population (standardized mean difference: 0.99; see Fig. 2 in Berner et al. 2010a), and this divergence coincides with distinct foraging modes: Lake Constance stickleback forage pelagically on zooplankton (Lucek et al. 2012; Moser et al. 2012), whereas their conspecifics from the CHE stream site feed on larger benthic macroinvertebrates (Berner et al. 2010a). Given that such concurrent divergence in gill raker length and prey utilization has also been found in other (lake-stream) stickleback systems (Gross and Anderson 1984; McPhail 1984; Schluter and McPhail 1992; Bolnick 2004; Berner et al. 2008, 2010a,b; Matthews et al. 2010; Ravinet et al. 2013), and even in distantly related fish species (Kahilainen and Ostbye 2006; Pfaender et al. 2011), the divergence between ROM and CHE stickleback is very likely adaptive. We note that benthic versus pelagic resource specialization often coincides with additional divergence in gill raker *number*, but because the source populations are not divergent in this trait (Berner et al. 2010a), we did not include this trait in the current analysis. Gill raker length was measured on the left first branchial arch of the preserved specimens under a stereomicroscope fitted with an ocular micrometer at 50× magnification (precision: 0.01 mm). We measured and then averaged the length of the rakers two to five (counted from the joint with the dorsal arch bone, see Berner et al. 2008).

Next, we considered two aspects of head morphology: snout length and overall head length (Fig. 1). The pelagic ROM lake population displays lower values for both traits relative to the

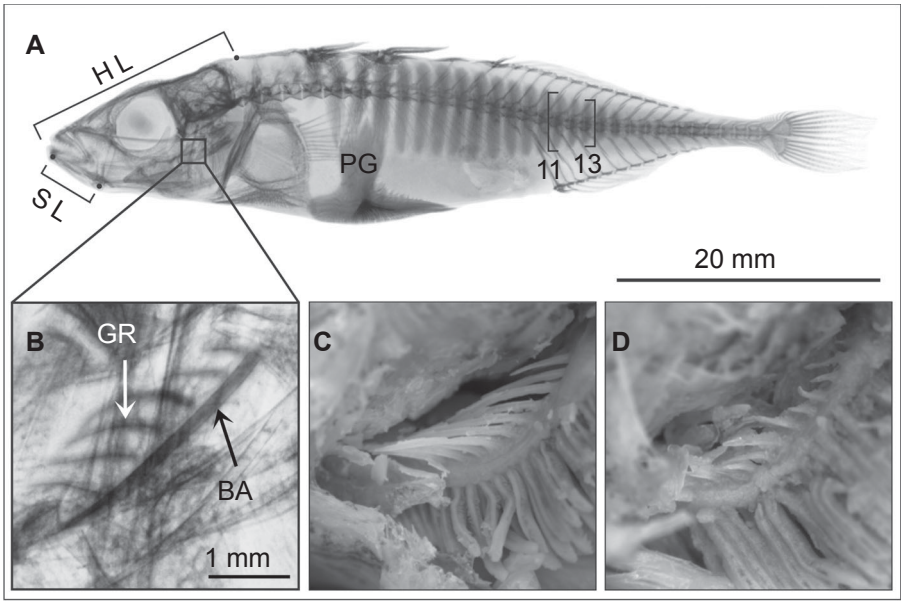

Figure 1. **Traits subjected to QTL mapping in lake and stream stickleback. (A) X-ray scan of a partially plated stickleback visualizing snout length (SL), head length (HL), the vertebrae, and the lateral plates. Plate height was measured on the plates 11 and 13 posterior to the pelvic girdle (PG). (B) Detail of the head, showing the gill rakers (GR) on the first lower branchial arch (BA). The subpanels (C) and (D) display, on the same scale as (B), the gill rakers of two size-matched individuals from the upper and lower end of the gill raker length distribution.**

CHE stream population foraging on benthic prey (Berner et al. 2010a), and similar foraging-related divergence is also seen in other stickleback systems (Caldecutt and Adams 1998; Albert et al. 2008). Moreover, head morphology typically shows sexual dimorphism (Caldecutt and Adams 1998; Kitano et al. 2007; Albert et al. 2008; Aguirre and Akinpelu 2010; Berner et al. 2010a, 2011; Ravinet et al. 2013). This dimorphism is possibly also related to differential foraging modes. The reason is that in stickleback, males tend a nest and provide parental care. The (presumably ancestral) necessity of males to forage on benthic resources during the breeding season while females can continue to exploit pelagic prey may have driven divergence in head structure between the sexes (Bentzen and McPhail 1984; Bentzen et al. 1984). Both snout length and head length were measured from the head X-ray scans. The former was defined as the distance from the joint to the tip of the lower jaw, the latter as the distance from the tip of the lower jaw to the dorsal posterior edge of the cranium.

The next trait quantified was vertebral number. Stickleback populations often differ in the number of vertebrae (Hagen and Gilbertson 1972; Moodie and Reimchen 1976; Reimchen et al. 1985). Although the functional basis of this variation remains poorly understood (but see Swain 1992), genetic analysis in stickleback may provide insights into vertebral diversification in other fish (Ward and Brainerd 2007; McDowall 2008) and vertebrates in general. As a first step, we thus produced whole-body X-ray scans of 14 specimens from each natural source population, counted all vertebrae excluding the urostyle (Fig. 1), and tested for a population difference in mean count using 9999 random permutations of the trait over the populations (Manly 2007; all significance testing in this study was performed using analogous permutation procedures). This analysis made clear that ROM stickleback have a higher number of vertebrae than CHE fish (see Results). Following the same methods, we therefore quantified vertebral number for the full F_2 panel. Because of skeletal anomalies, 18 individuals could not be scored unambiguously, leaving 474 datapoints.

Finally, our phenotypic analysis included elements of lateral plating. Ancestral marine stickleback display a complete series of bony plates along their body, whereas the number of plates is typically greatly reduced in freshwater populations (Bell and Foster 1994). This difference is presumably attributable to differential exposure to predators (Hagen and Gilbertson 1972; Reimchen 1994; Bergstrom 2002; Leinonen et al. 2011a), although other ecological factors targeting plate number or other traits correlated with plate number due to pleiotropy or genetic linkage might influence plate evolution as well (e.g., Heuts 1947; Giles 1983; Barrett et al. 2009; Myhre and Klepaker 2009; Leinonen et al. 2011b; Roesti et al. 2014). Interestingly, Lake Constance stickleback are a rare example of a freshwater population almost completely fixed for the fully plated phenotype (Berner et al. 2010a; Moser et al. 2012). Because plating is reduced in several tributary streams to Lake Constance, the persistence of full plating in the lake likely reflects an adaptation to high predator exposure associated with a pelagic life style. By contrast, CHE stickleback represent a

typical low-plated freshwater population (Berner et al. 2010a), thus providing the opportunity to map variation in lateral plating in the F_2 cross. Consistent with previous work (Berner et al. 2010a; Moser et al. 2012), we scored the extent of lateral plating using three discrete phenotypic classes (low, partially, and fully plated).

Previous mapping efforts and subsequent functional analysis in Pacific marine and freshwater stickleback have already identified the *Ectodysplasin* (*EDA*) gene as a major driver of evolutionary shifts in the extent of lateral plating (Colosimo et al. 2004, 2005; Cresko et al. 2004; Baird et al. 2008). Moreover, targeted sequencing of the entire *EDA* coding region revealed distinct haplotypes in fully plated Lake Constance versus low-plated CHE stream fish (Berner et al. 2010a). Our primary objective in mapping plate morph was therefore to assess if genomic regions beyond *EDA* contribute to plating divergence between these European freshwater populations. To this end, we additionally counted the total number of lateral plates posterior to the pelvic girdle (including the plates forming the caudal keel) across both body sides in the subset of F_2 individuals genotyped unambiguously as heterozygotes at our single SNP marker located within *EDA*. Focusing on this particular subset ($N = 209$) allowed us to screen for loci influencing the extent of plating while controlling rigorously for the effect of the known major locus.

As an alternative to reducing the extent of lateral plating via a reduction in the *number* of plates (see above), stickleback sometimes appear to evolve *shallower* plates (Leinonen et al. 2012). Although differences in plate size between ROM and CHE stickleback could not be examined adequately because the latter are low-plated, a preliminary inspection of the F_2 population indicated substantial variation in plate height. We therefore measured the maximal height of the plates 11 and 13, as counted from the pelvic girdle, perpendicular to the anterior-posterior axis on the left body side (Fig. 1). Measurements were taken with a digital caliper (precision: 0.01 mm) handled under a stereomicroscope at 10–30× magnification. As plate height could only be quantified in the fully and most of the partially plated individuals, sample size was 358 and 342 for plate 11 and 13.

All metric (length) traits considered in our study scaled strongly with overall body size (Pearson's r: 0.49–0.84), whereas the meristic (count) traits did not (vertebral number: $r = 0.042$; lateral plate number: $r = 0.045$). Prior to QTL mapping, we therefore subjected the former traits to size correction by regressing each trait separately against body size, and treating the residuals as size-independent variables (Reist 1985; Berner 2011). These variables were shifted back into the original measurement range by adding the trait value predicted by the regression at mean body size across all individuals. To obtain a robust size metric for these procedures, we used tpsDig (Rohlf 2001) to digitize 16 landmarks as described in Berner et al. (2010a) on the digital photographs of all individuals, and extracted geometric morphometric centroid size using TpsRelw (Rohlf 2001).

Finally, we assessed measurement precision for all traits by remeasuring 30 haphazardly selected individuals on a second occasion, and calculating the repeatability (Lessells and Boag 1987). Repeatability was consistently very high, ranging from 0.96 (plate number) to 1 (vertebral number, plate morph). The complete phenotype matrix used for mapping in R/qtl is available on the Dryad Digital Repository (doi:10.5061/dryad.b2534).

MARKER GENERATION

As markers for mapping, we used single nucleotide polymorphisms (SNPs) discovered by RAD sequencing (Baird et al. 2008). In brief, this involved DNA restriction with the *Sbf1* enzyme, and sequencing pools of 62 barcoded individuals in eight lanes with 100 cycles on an Illumina HiSeq 2000 instrument. RAD library preparation and the bioinformatics pipeline used for SNP discovery and genotyping were exactly as described in Roesti et al. (2013). From the 2165 markers thus obtained, we excluded 154 to avoid *Sbf1* restriction sites being represented by more than one SNP. We also discarded four individuals exhibiting more than 10% missing genotypes across all markers. Our final mapping dataset thus comprised 488 F_2 individuals (recall that sample size was lower for some traits) and 2011 SNPs. The genotype matrix used for mapping is available on the Dryad Digital Repository (doi:10.5061/dryad.b2534).

QTL MAPPING

All SNPs were ordered physically according to the stickleback genome reassembly performed in Roesti et al. (2013; available at http://datadryad.org/resource/doi:10.5061/dryad.846nj.2), resulting in 61–152 markers per chromosome and a median marker spacing of 118 kb. Next, we excluded 111 individuals with relatively low genotyping quality, as judged by clearly inflated genome-wide crossover count (we here used 2.5 times the median autosomal crossover count across all 488 individuals as threshold). The remaining 377 individuals were used to estimate the genetic map in R/qtl (Broman and Sen 2009), applying the Kosambi map function (assuming crossover interference). The resulting genetic map proved highly consistent with that provided in Roesti et al. (2013) based on fewer individuals but with genotype errors corrected manually, and was used to specify the genetic marker distances for QTL mapping. Mapping with genetic distances estimated by using the full F_2 panel produced very similar results (details not presented).

All phenotypes were subjected to single-QTL interval mapping in R/qtl using the extended Haley–Knott regression method (Broman and Sen 2009) and the full F_2 panel. Head length was mapped both with and without snout length entered as covariate, as our head length measure included the snout tip. We present

the former analysis only, noting that both approaches produced quantitatively very similar results. QTL significance was established based on the distribution of genome-wide maximum LOD (logarithm of the odds ratio for QTL likelihood) scores scores across 1000 random permutations of the phenotype data over the genotype data (Broman and Sen 2009). In the Results, we present only QTLs significant at the 0.05 level, but additional loci are considered in the Discussion, and a table including suggestive QTLs ($0.05 \leq P < 0.1$) is provided as Table S1. QTL effect sizes were quantified both as the percentage of the total phenotypic variance in the F_2 cross explained by the QTLs (percent variance explained, PVE), and as their allelic substitution effect (i.e., the phenotypic difference between the two homozygous genotype classes). We present the latter both in the traits' original measurement scale (millimeter for all length traits), and standardized by the average standard deviation within the homozygous genotype classes. All statistics and plotting were carried out with the R language (R Development Core Team 2013).

EXPLORING QTLs

Following QTL detection, we retrieved from the Ensembl Genome Browser all genes located in the physical window spanned by the two SNPs flanking the marker displaying the LOD peak (this interval usually coincided with the 1.5 LOD support interval). We then scanned these gene lists for strong causative candidates, as judged by information on protein function in vertebrate model organisms (chicken, mice, rats, humans) compiled in the UniProt database (The UniProt Consortium 2013).

In addition, the availability of RAD sequences generated previously for the ROM and CHE population allowed us to inspect the magnitude and direction of allele frequency shifts in the wild at QTLs discovered in the F_2 population. Although this type of follow-up analysis has, to our knowledge, not previously been carried out, it promised stronger QTL inference because a genotype–phenotype association shared between a cross and its natural source populations suggests that the focal QTL is effectively contributing to divergence in the wild, as opposed to being specific to the cross. As a caveat, we note that this approach assumes that the tight linkage detected between marker and QTL alleles in the cross also persists in the wild. Specifically, we here capitalized on RAD sequence data from 27 individuals sampled from each source population. Details on the wet laboratory protocol, the analysis pipeline, and access to the sequence data are provided in Roesti et al. (2012b; this reference describes data generation for the ROM population only; the CHE dataset has not previously been analyzed but was generated in exactly the same way). Because the RAD libraries of both the cross and the natural populations were generated using the *Sbf1* restriction enzyme, all RAD loci of interest were shared among the two datasets. However, the latter libraries were Illumina-sequenced to 76 bases as opposed to 100 bases for the cross, thus precluding the examination of allele frequencies in the natural populations at QTL-linked SNPs located distal to the restriction site. We further ignored SNPs linked to lateral plate height QTLs because we here lacked information on the direction and magnitude of divergence between the natural populations (see above).

For those SNPs represented in both the cross and the natural population datasets (four SNPs in total), we first determined from which population each of the two alleles present in the cross originated. This assignment was unambiguous because our study considered only markers homozygous within each grandparent (Roesti et al. 2013). Next, we arbitrarily converted the two alleles to integers (0, 1) and tested for frequency shifts by random permutation, using the difference in the population means as test statistic. While providing a formal test for population divergence at QTL-linked SNPs, this approach yielded no information regarding the potential cause of divergence at these SNPs. To gain insights into the latter, we performed a second analysis comparing the SNP allele frequency shifts between the natural populations to the magnitude of genome-wide baseline divergence between the populations. The rationale was that an allele frequency shift clearly exceeding baseline divergence—reflecting the magnitude of differentiation by drift—offers evidence for divergent selection having acted in the close neighborhood of the QTL-linked marker. We recognize the possibility, however, that selection may not have target the detected QTL itself, but a nearby locus unrelated to the mapped phenotype.

We thus translated allele frequency differences at the QTL-linked SNPs to F_{ST} (Nei and Tajima 1981, eq. 7), and estimated the confidence interval for F_{ST} as the 95 percentile of the distribution produced by bootstrap resampling the observed alleles 10,000 times within each population (Manly 2007). This confidence interval was then evaluated against the magnitude of baseline differentiation between the ROM and CHE population samples, defining baseline differentiation as genome-wide median F_{ST} (Roesti et al. 2012a). Following Roesti et al. (2012a,b), the estimation of baseline differentiation ignored SNPs with a minor allele frequency <0.25 to avoid polymorphisms with low information content, and for RAD sites harboring multiple polymorphisms used only the one SNP yielding the highest F_{ST} value. Baseline differentiation thus calculated was 0.37 across 5429 informative SNPs.

Results

GILL RAKER LENGTH

We found two significant QTLs influencing gill raker length (Table 1; an additional suggestive QTL is described in Table S1;

Table 1. Characterization of the QTLs for skeletal divergence between lake and stream stickleback.

Trait	Marker	Chromosome	Position (bp)	LOD	*P*	PVE	HSE	Direction	Candidate gene
Gill raker length	chrVI_12733534	6	13,735,445	4.52	0.027	6.5	0.19 (0.73)	L*	
	chrIV_570692	4	570,692	4.60	0.019	4.3	0.08 (0.33)	S	*BAPX1* (15)
Snout length	chrXIX_19432535	19	69,077 (contig 1730)	45.13	0.001	42.9	0.38 (1.87)	M	
Head length	chrXIX_19432535	19	69,077 (contig 1730)	5.70	0.002	7.7	0.33 (0.58)	M	
	chrUn_11709633	5	464,792	5.57	0.004	6.9	0.45 (0.72)	S*	
	chrXV_11777081	15	11,777,081	5.01	0.015	4.4	0.38 (0.58)	S*	
	chrXIV_6849438	14	6,849,438	4.55	0.031	3.2	0.24 (0.37)	S*	
Vertebral number	chrXXI_2306628	21	4,955,041	7.82	0.001	9.2	0.43 (0.85)	L*	*COL11A1* (6)
	chrXVII_1670571	17	1,670,571	7.64	0.001	6.4	0.44 (0.78)	L*	*ASPN, OGN* (11)
Plate morph	chrIV_12797213	4	12,797,213	155.45	0.001	76.0	–	L*	*EDA* (15)
Plate 11 height	chrXI_10140558	11	10,140,558	9.69	0.001	12.7	0.79 (1.04)	S	*AXIN2* (36)
	chrXI_6239999	11	6,239,999	8.94	0.001	12.0	0.71 (0.97)	S	*PHOSPHO1* (36)
	chrIV_4185607	4	4,185,607	4.54	0.041	5.5	0.47 (0.6)	L	
Plate 13 height	chrIV_6474941	4	6,474,941	8.20	0.001	11.8	0.58 (1.07)	L	
	chrXI_10140558	11	10,140,558	5.96	0.002	9.4	0.6 (0.8)	S	*AXIN2* (36)
	chrXI_6239999	11	6,239,999	5.79	0.002	8.4	0.47 (0.69)	S	*PHOSPHO1* (36)
	chrIX_9659641	9	12,543,749	4.99	0.012	7.7	0.53 (0.71)	L	

The marker names specify genomic locations (chromosome and base pairs) according to the Broad S1 genome assembly, whereas the chromosome numbers and positions given in separate columns refer to the improved assembly (Roesti et al. 2013). The position of the marker on chromosome 19 (sex chromosome) is unclear (it proved linked relatively loosely to the other markers within the nonrecombining domain of this chromosome), hence we provide the position within its contig. Effect sizes are expressed as percent variance explained (PVE), and as homozygous substitution effect (HSE; in measurement unit, and standardized in parentheses). HSE is not given for plate morph, as this trait has an ordinal scale, and effect sizes for the two plate height QTLs on chromosome 11 are probably inflated because of linkage. The QTLs are ordered by PVE within each trait. The Direction column indicates whether ROM lake (L), CHE stream (S), or male (Y-linked; M) alleles cause higher trait values, and asterisks indicate allelic effects in the direction expected from the divergence between the natural populations (note that this could not be determined for the plate height QTL). The last column lists candidate genes found in the marker intervals around the QTL SNPs, with the numbers in parentheses indicating the total number of genes in each interval (including predicted genes). This table reports only QTLs reaching $P < 0.05$; additional suggestive loci are presented in Table S1.

genome-wide LOD profiles for all traits are presented as Fig. S1). Both showed a modest effect size. The SNP associated with the QTL exhibiting the greater effect size (located on chromosome 6) produced a phenotypic shift in the predicted direction (longer gill rakers associated with the ROM lake allele), while the other one did not. Only the chromosome 6 marker could be analyzed for allele frequency shifts in the natural populations, revealing almost complete fixation of the expected SNP allele within the ROM and CHE sample (permutation $P = 0.0001$). This frequency shift ($F_{ST} = 0.77$, lower and upper 95% confidence limits: 0.65, 0.92) was much stronger than expected from the populations' baseline divergence.

HEAD MORPHOLOGY

The analysis of snout length detected a single large-effect QTL only (43 PVE; Table 1, Fig. S1). This QTL mapped to the domain on the sex chromosome (19) where the X and Y gametologs do not recombine (Roesti et al. 2013). Males of the F_2 population further displayed strikingly longer snouts than females (Fig. 2). Together, these observations indicated very strong sex-linked control of snout length. Indeed, mapping sex as a binary trait produced a single significant QTL (LOD = 380) coinciding exactly with the snout length QTL, whereas mapping snout length separately within each sex produced no QTL (details not presented).

Some sex-linked control was observed for overall head length as well, as the snout length QTL was also the strongest QTL affecting head length (Tables 1, S1, Fig. S1; recall that head length was mapped with snout length as covariate, so this finding is not a methodological artifact). Three additional minor head length QTLs were detected on the autosomes, all of them (and also the suggestive locus) exhibiting an effect in the direction predicted from previous phenotypic work (a larger head associated with the CHE stream alleles). Allele frequencies in the natural populations could be inspected for the marker linked to the QTL on chromosome 15 only, which again revealed a shift in the predicted direction ($P = 0.0001$; $F_{ST} = 0.51$, CLs: 0.35, 0.68) and exceeding the baseline level.

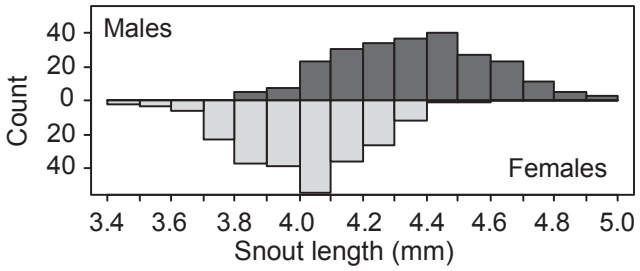

Figure 2. Distribution of size-adjusted snout length in male (dark gray, pointing upward) and female (light gray, pointing downward) stickleback from the F_2 panel.

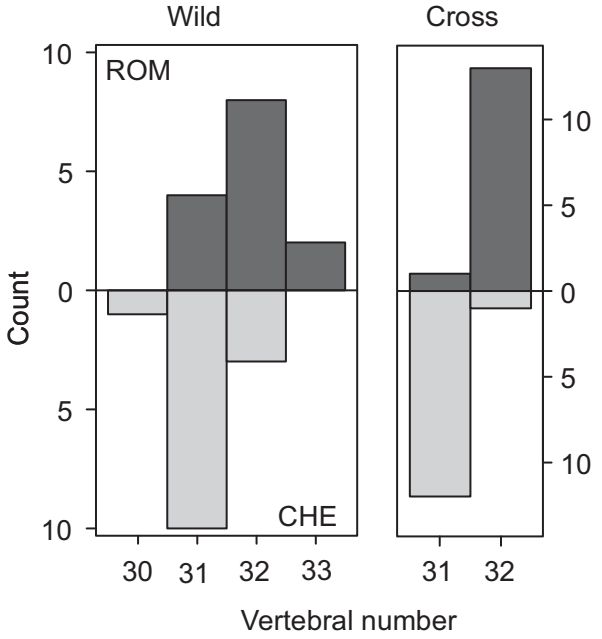

Figure 3. Vertebral number in ROM lake and CHE stream stickleback. The left panel shows vertebral count histograms based on a sample ($N = 14$) from the lake population (dark gray, pointing upward) and the stream population (light gray, pointing downward). The right panel displays the distribution of vertebral number in individuals from the F_2 cross concurrently homozygous for either the lake alleles (dark gray; $N = 14$) or the stream alleles (light gray; $N = 13$) at the two QTLs identified on chromosomes 17 and 21.

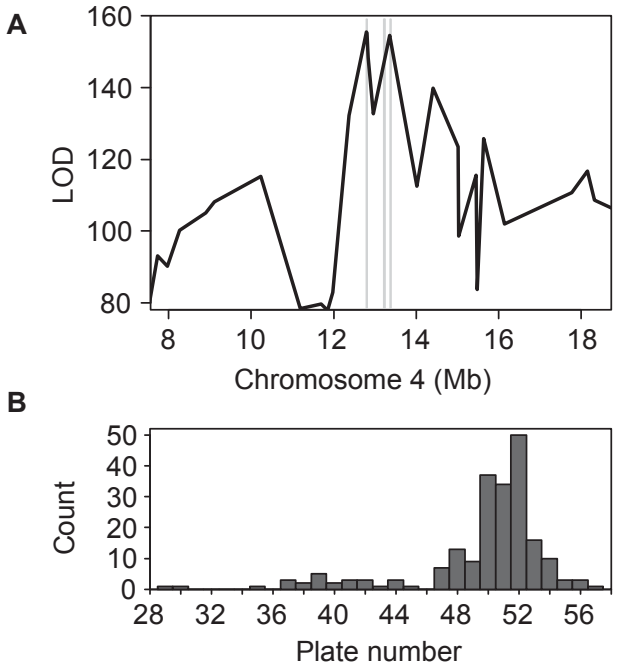

Figure 4. (A) LOD profile for the segment on chromosome 4 containing the detected QTL for lateral plate morph. The gray vertical lines indicate, from left to right, the position of *EDA* and the two candidate genes *PDLIM7* and *ANXA6*. The two LOD peaks (>150) are separated by two markers. (B) Distribution of the total number of lateral plates posterior to the pelvic girdle in F_2 individuals heterozygous at the *EDA* marker.

VERTEBRAL NUMBER

Most stickleback from the ROM lake sample displayed 32 vertebrae, as opposed to 31 vertebrae predominating in CHE stream fish ($P = 0.0085$; Fig. 3). In the cross, vertebral number mapped to two QTLs, with their effects being in the expected direction (ROM lake alleles associated with greater vertebral number; the same is true for the suggestive loci; Tables 1, S1, Fig. S1). Despite moderate effect sizes of the two QTLs when estimated separately (9.2 and 6.4 PVE), their joint effect was striking: individuals homozygous for the ROM lake or CHE stream alleles at both QTL-linked SNPs simultaneously exhibited almost consistently 32 versus 31 vertebrae (Fig. 3). Comparing a subset of F_2 individuals with 31 and 32 vertebrae ($N = 30$ each) showed unambiguously that the variation was in the number of caudal as opposed to abdominal vertebrae (details not presented). Moreover, testing for a difference in mean body size between individuals with 31 versus 32 vertebrae (together accounting for 97% of all F_2 individuals) revealed clearly that vertebral number and body size were unrelated ($P = 0.36$, standardized mean difference in size between the two groups: 0.06; visualized in Fig. S2). Allele frequency shifts could be examined for the marker linked to the QTL on chromosome 21 only, revealing divergence in the expected direction ($P = 0.0001$; $F_{ST} = 0.41$, CLs: 0.15, 0.71), but not stronger than expected from the baseline.

LATERAL PLATING

Mapping lateral plate morph detected a locus of large effect (76 PVE) on chromosome 4, located precisely in the *EDA* region (LOD = 155.4 for the SNP 3 kb from the start position of *EDA*, and LOD = 155.2 for the SNP within *EDA*; Table 1, Fig. 4A). An almost equally strong marker-phenotype association (LOD = 154.6), however, occurred at 13.35 Mb. Inspecting the genotype frequencies at the two SNPs separating these high-LOD regions indicated that the drop in the strength of marker-phenotype association was not due to low genotyping quality (details not presented). At the *EDA* SNP, the natural populations were relatively close to fixation for the expected alternative alleles ($P = 0.0001$; $F_{ST} = 0.60$, CLs: 0.42–0.79), a shift clearly exceeding the baseline divergence level. No additional plate morph QTL was found (Fig. S1).

Lateral plate number was variable among the F_2 individuals heterozygous at *EDA*, but never lower than 29 (Fig. 4B). Hence, *EDA* heterozygotes in our cross always classified as either partially or fully plated. We found no significant QTL for plate

number when only considering *EDA* heterozygotes (Fig. S1; a single suggestive QTL is described in Table S1).

The height of lateral plate 11 mapped to two QTLs (Tables 1, S1, Fig. S1). The locus on chromosome 11 displayed a substantial effect size (12.7 PVE), with the ROM lake allele associated with shorter plates. However, this effect size was probably slightly inflated, as inspecting the LOD profile along chromosome 11 revealed the presence of an additional, nearly equally strong QTL 4 Mb (9.4 cM) away (LOD = 8.94; this second QTL is included in Table 1). Lacking information on plate height divergence between the natural populations, we did not investigate population-level shifts in allele frequencies.

The genetic architecture of lateral plate 13 height overlapped partly with that of plate 11 (Table 1, Fig. S1), which is not surprising, given the relatively strong phenotypic correlation of the two plate height traits within the F_2 population ($r = 0.84$). Specifically, we detected exactly the same two QTLs located on chromosome 11. However, the strongest effect (11.8 PVE) was now seen in a QTL on chromosome 4. This locus was 2.3 Mb away from the QTL on the same chromosome driving plate 11 height (Fig. S1), and thus perhaps represents a distinct locus, although this cannot be determined with confidence. In addition, plate 13 height was influenced by a QTL on chromosome 9.

Discussion

We have used an F_2 intercross to investigate the genetic architecture of divergence in skeletal traits between lake and stream stickleback. A first suite of traits considered included gill raker, snout, and head length, traits believed to mediate trophic specialization. In particular, gill raker length displays a highly predictable association with prey use in stickleback and other fish species. To our knowledge, variation in gill raker length has not previously been mapped in any species, but common-garden experiments in stickleback indicated a heritable basis to the phenotypic divergence between benthic and pelagic populations (McPhail 1984; Day et al. 1994; Wund et al. 2008). In line with these quantitative genetic observations, our study discovered QTLs for gill raker length. Despite a mutation screen in zebrafish, implicating the *Ectodysplasin* (*EDA*) signaling pathway in gill raker formation (Harris et al. 2008), the detected QTLs showed no obvious relationship to that pathway. However, screening the marker interval around the QTL on chromosome 4 suggested *BAPX1* as a strong candidate gene, given that *BAPX1* is crucial to the formation of the first branchial arch in zebrafish (Miller et al. 2003).

We also found several autosomal QTLs explaining variation in head length. The effect sizes were consistently in the direction expected from the phenotypic divergence between the source populations (Berner et al. 2010a) and other benthic-pelagic stickleback systems (Caldecutt and Adams 1998; Albert et al. 2008). Nevertheless, in accordance with greater male than female overall head length found in many stickleback studies (Caldecutt and Adams 1998; Kitano et al. 2007; Albert et al. 2008; Aguirre and Akinpelu 2010; Berner et al. 2010a, 2011; Ravinet et al. 2013), the strongest head length QTL was sex-linked and also turned out to be the only (large-effect) locus driving snout length. Hence, while contrasting foraging habitats likely drive the evolution of stickleback head morphology among populations, the footprint of sex-specific selection is much stronger.

VERTEBRAL NUMBER

The source populations of the cross showed clear divergence in the number of vertebrae, with a higher average count in lake than stream fish. This trend has also been found in other studies comparing lake and stream stickleback (Hagen and Gilbertson 1972; Reimchen et al. 1985) and thus likely represents an adaptive response to divergent selection on locomotion (Swain 1992). Although further functional evidence is needed, our finding that vertebral number is genetically unrelated to body size (as also found in a different stickleback system; Alho et al. 2011) indicates that population divergence in the number of vertebrae is unlikely to reflect a correlated response to selection on size (note that the ROM lake and CHE stream populations differ in size; Moser et al. 2012).

In our cross, vertebral number mapped to two QTLs. These loci explained a moderate proportion of the total phenotypic variance when considered in isolation, but in combination had a high explanatory power: their joint homozygous substitution accounted for an approximate shift of one vertebra, roughly the magnitude of divergence between the natural populations. To our knowledge, vertebral number has previously been mapped only in two fish species (medaka and trout) and in pigs. The former studies detected QTLs but were performed with a marker resolution too low to allow candidate gene identification (Nichols et al. 2004; Kimura et al. 2012). QTLs also emerged in pigs, where fine mapping produced strong candidate genes (*NR6A1*, *VRTN*, *PROX2*, *FOS*; Mikawa et al. 2007, 2011; Ren et al. 2012). The stickleback homologues of these genes, however, are not located on the chromosomes 17 and 21 where we found QTLs for vertebral number. Instead, screening the target marker interval on chromosome 17 identified *OGN* (Madisen et al. 1990) and *ASPN* as candidate genes. Both genes are involved in bone formation. In particular, *ASPN* regulates osteoblast collagen mineralization *in vitro* (Kalamajski et al. 2009) and is implicated in human degenerative diseases of skeletal joint regions, including intervertebral disks (Kizawa et al. 2005; Song et al. 2008). Also, a strong candidate gene (*COL11A1*) emerged in the focal chromosome 21 segment. Mutations in *COL11A1* cause skeletal disorders, including the malformation of vertebrae (Li et al. 1995; Tompson et al. 2010; Koyama et al. 2012).

LATERAL PLATING

At first glance, our mapping of lateral plate morph produced an expected result: the LOD maximum mapped to the *EDA* gene, and the corresponding SNP explained 76% of the total variance, a value very similar to that reported in Colosimo et al. (2004) for the plate morph QTL on chromosome 4 (77.6 PVE). Interestingly, however, a nearly equally strong LOD score emerged at 13.35 Mb (roughly 0.5 Mb from *EDA*), a region identified as high differentiation outlier in a divergence mapping study using fully plated marine and low-plated freshwater stickleback from Alaska (Hohenlohe et al. 2010). Our marker interval in that region contains two strong candidate genes, *PDLIM7* and *ANXA6* (see also Hohenlohe et al. 2010). *PDLIM7* has been shown to initiate bone formation de novo, and also to interact with bone morphogenetic protein (*BMP*) signaling (Boden et al. 1998; Liu et al. 2002). Similarly, *ANXA6* plays a critical role during the calcification of skeletal tissue (Kirsch et al. 2000; Wang and Kirsch 2002; Thouverey et al. 2009). It is thus possible that the strong effect seen at the *EDA* marker in our cross captures variation in lateral plating driven by polymorphism in one or more additional genes in its close neighborhood. Unfortunately, the paucity of crossovers between the SNPs at these QTLs in our cross precludes disentangling their relative effect sizes.

Outside chromosome 4, we found no QTL substantially influencing plate morph or number. This is surprising, given that such QTLs were discovered previously on chromosomes 7, 10, and 21 (Colosimo et al. 2004; but see Baird et al. 2008). This difference in genetic architecture likely explains why *EDA* heterozygotes in our cross were never low-plated, although low-plated heterozygotes occurred in the mapping panel studied by Colosimo et al. (2004).

As a complementary route to the adaptive reduction in lateral plating, stickleback might evolve shallower plates (Leinonen et al. 2012). Mapping the height of the plates 11 and 13 posterior to the pelvic girdle, we found QTLs on chromosomes 4, 9, and 11. These results differ from the previous report of plate height QTLs on the chromosomes 4 (at around 2 Mb, hence in a different region than in our cross), 7, and 20 (Colosimo et al. 2004). However, that study measured plates immediately adjacent to the pelvic girdle. Combined with our observation that the relative influence of the QTLs on chromosomes 4 and 11 on the height of the plates 11 and 13 was inverted, and that the QTL on chromosome 9 (and the additional suggestive QTLs) influenced one of the plates only, we conclude that plate height has a fairly complex genetic architecture, with several loci acting relatively locally.

Examining the plate height QTL regions produced strong candidate genes. Notably, the marker interval around the highest LOD peak observed (chromosome 11) included *AXIN2*. Loss of function mutations in *AXIN2* lead to ectodermal dysplasia in humans (Lammi et al. 2004; Mostowska et al. 2006; Callahan et al. 2009; Bergendal et al. 2011)—the same disorder also observed for disruptions of the *EDA* pathway (Kere et al. 1996; Bayes et al. 1998; Monreal et al. 1999; Headon et al. 2001; Chassaing et al. 2006). The SNP interval around 6.2 Mb on the same chromosome, in turn, proved close to *PHOSPHO1*, a gene involved in skeletal tissue mineralization (Houston et al. 1999, 2004; Roberts et al. 2007). Candidate genes involved in bone formation also emerged at the suggestive plate height QTLs on chromosomes 5 (*PLEKHM1*; Van Wesenbeeck et al. 2007) and 17 (*ALPL*; Weiss et al. 1988; Henthorn et al. 1992; Table S1).

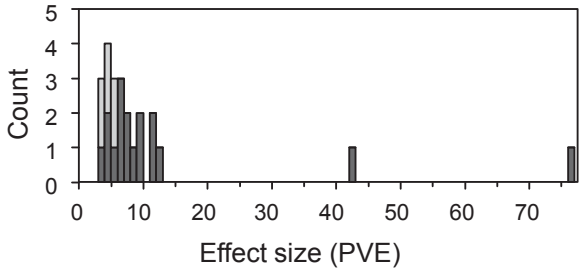

Figure 5. Distribution of effect sizes (in percent variance explained) across all QTLs (including in light gray the suggestive ones with $0.05 \leq P < 0.1$; see Table S1) and all traits except plate number in *EDA* heterozygotes. The latter trait was excluded because mapping was performed with substantially reduced power ($N = 209$).

QTL EFFECT SIZES

Mapping lateral plate morph and snout length identified QTLs of very large effect (acknowledging that the effect size of the plate morph QTL is possibly confounded by the presence of multiple tightly linked loci, see above). The majority of our detected QTLs, however, had a relatively minor effect, a typical result in QTL mapping studies (Mackay et al. 2009). Moreover, for some traits (e.g., gill raker length, head length), inspecting the genome-wide LOD profile (Fig. S1) suggested the presence of additional loci with even smaller effect that were missed in our experiment due to insufficient power—a well-known issue in QTL mapping (Lande and Thompson 1990; Beavis 1994; Xu 2003; Rockman 2011). To explore this issue further, we compiled the effect sizes of all the QTLs (including marginally significant ones) detected in our study across all traits. This revealed that despite relatively large F_2 sample size, we lacked the power to identify QTLs with an effect size below 3–4 PVE (Fig. 5). (We are aware of the additional complication that the effect sizes of our detected *minor* QTLs are likely to be biased upward; Beavis 1994; Göring et al. 2001; Xu 2003.) We thus argue that although QTL mapping provides interesting insights into the genetic architecture of phenotypic divergence among stickleback populations, our understanding of adaptive variation in many traits will continue to benefit from quantitative genetic investigation.

ALLELE FREQUENCY SHIFTS IN THE SOURCE POPULATIONS

The availability of marker data from the natural populations underlying our cross made it possible to assess if associations between trait values and QTL-linked SNP alleles were replicated at the population level. Such an association is expected under two conditions. First, SNP alleles must tag QTL alleles reliably at the population level (as opposed to merely in the grandparents used for the cross). Second, allele frequency shifts at the focal QTL need to make some contribution to the trait divergence between the natural populations. Moreover, a shift at an SNP tightly linked to a QTL is expected to exceed the level of baseline population divergence attributable to drift if the QTL has been influenced by divergent selection between the populations.

All these conditions are indeed met by the *EDA* locus: phylogenetic analysis revealed that alleles at SNPs within *EDA* are tightly linked to their corresponding causative variants (which remain unknown) in the two study populations, and that adaptive population divergence in plate morph frequency is paralleled by frequency shifts at these SNPs (Berner et al. 2010a; see also Colosimo et al. 2005). We thus predicted very strong population-level shifts at our *EDA* maker, which were indeed observed. Similar analyses could be performed only in a small subset of the other QTL-linked SNPs, because some relevant markers were missing at the population level due to a different sequencing protocol, and because plate height could not be quantified in the (low-plated) stream population. Nevertheless, all three additional SNPs that were examined (associated with gill raker length, head length, and vertebral number) showed clear enrichment for the expected allele within each source population. Moreover, in three of the four total cases (including *EDA*), the observed allele frequency shifts were stronger than baseline divergence. We thus conclude that the phenotypic divergence between our study populations is probably attributable at least partly to allele frequency shifts at the QTL discovered in the cross, and that some of these shifts have been driven by divergent selection.

Conclusions

We subjected skeletal traits in European lake and stream stickleback to QTL mapping. Although this revealed a few large-effect QTLs, the majority of the loci detected across all traits exhibited a modest to small effect size. At least for some traits, QTL mapping seems to permit a relatively incomplete characterization of genetic architecture. Nevertheless, the close neighborhood around the QTLs that were discovered often contained genes involved in bone formation, which thus emerge as strong candidate drivers of skeletal evolution. Manipulative functional experiments are now needed to confirm the causative role of these genes, and comparisons across numerous phenotypically well-characterized stickleback populations should investigate how consistently these genes are involved in diversification. Excitingly, a region containing two novel candidate genes for lateral plate morph evolution in our study coincided with an outlier region identified in a divergence scan using geographically independent stickleback populations divergent in lateral plating (Hohenlohe et al. 2010). This illustrates how understanding adaptation can benefit from the combination of phenotype-based and purely molecular genome scans. Finally, we attempted to move beyond mere QTL identification within a cross by screening for QTL-linked SNP allele frequency shifts in the natural source populations. These analyses indicated that at least some of our identified QTLs may indeed contribute to population divergence, and suggested that allele frequency shifts have been driven by divergent selection. A deeper understanding of the nature of this selection, however, will require extensive ecological investigation.

ACKNOWLEDGMENTS

We gratefully acknowledge the following contributions: W. Cresko and C. Peichel provided input on the cross and marker generation design. F. Hofmann (SFFN—Inspection de la pêche VD) and R. Kistler (fisheries authorities of the canton Thurgau) provided sampling permits for the cross populations, and A.-C. Grandchamp aided field sampling. B. Egger, H. Gante, A. Indermaur, A. Theis, and P. Vonlanthen aided fish husbandry. X-ray scanning was supported by the group of M. Kneissel, Global Head Musculoskeletal Disease Area, Novartis Institutes for BioMedical Research, Basel, Switzerland. L. Bänziger, A. Frey, B. Kueng, and S. Moser carried out preliminary analyses. B. Aeschbach and N. Boileau facilitated wet laboratory work. Illumina sequencing was done by I. Nissen and C. Beisel at the Quantitative Genomics Facility, D-BSSE, ETH Zürich. Novocraft (http://www.novocraft.com) shared their sequence aligner. J. Merilä, C. Peichel, and an anonymous reviewer provided valuable comments on the manuscript. This study was funded by the Swiss National Science Foundation (grant 31003A_146208/1 and Ambizione fellowship PZ00P3_126391/1 to DB; Sinergia grant CRSII3_136293 to WS), the Freiwillige Akademische Gesellschaft (FAG) Basel (DB), and the Research Fund of the University of Basel (DB, WS). DB designed the study, produced the cross, measured phenotypes, generated the genotype data, performed all mapping, and wrote the paper, with input from all coauthors. DM contributed to fish husbandry. DM and MR did the molecular wet lab work and measured phenotypes. MR contributed to study design and did the candidate gene search. HB generated all X-ray scans. WS contributed to study design and provided resources and infrastructure.

DATA ARCHIVING

The doi for our data is 10.5061/dryad.b2534.

LITERATURE CITED

Aguirre, W. E. 2009. Microgeographical diversification of threespine stickleback: body shape-habitat correlations in a small, ecologically diverse Alaskan drainage. Biol. J. Linn. Soc. 98:139–151.

Aguirre, W. E., and O. Akinpelu. 2010. Sexual dimorphism of head morphology in threespine stickleback (*Gasterosteus aculeatus*). J. Fish Biol. 77:802–821.

Akey, J. M., G. Zhang, K. Zhang, L. Jin, and M. D. Shriver. 2002. Interrogating a high-density SNP map for signatures of natural selection. Genome Res. 12:1805–1814.

Albert, A. Y. K., S. Sawaya, T. H. Vines, A. K. Knecht, C. T. Miller, B. R. Summers, S. Balabhadra, D. M. Kingsley, and D. Schluter. 2008. The genetics of adaptive shape shift in stickleback: pleiotropy and effect size. Evolution 62:76–85.

Alho, J. S., T. Leinonen, and J. Merilä. 2011. Inheritance of vertebral number in the three-spined stickleback (*Gasterosteus aculeatus*). PLoS One 6:e19579.

Arendt, J., and D. Reznick. 2008. Convergence and parallelism reconsidered: what have we learned about the genetics of adaptation? Trends Ecol. Evol. 23:26–32.

Baird, N. A., P. D. Etter, T. S. Atwood, M. C. Currey, A. L. Shiver, Z. A. Lewis, E. U. Selker, W. A. Cresko, and E. A. Johnson. 2008. Rapid SNP discovery and genetic mapping using sequenced RAD markers. PLoS One 3:e3376.

Barrett, R. D. H., S. M. Rogers, and D. Schluter. 2009. Environment specific pleiotropy facilitates divergence at the *ectodysplasin* locus in threespine stickleback. Evolution 63:2831–2837.

Barton, N. H., and P. D. Keightley. 2002. Understanding quantitative genetic variation. Nat. Rev. Genet. 3:11–21.

Bayes, M., A. J. Hartung, S. Ezer, J. Pispa, I. Thesleff, A. K. Srivastava, and J. Kere. 1998. The anhidrotic ectodermal dysplasia gene (EDA) undergoes alternative splicing and encodes ectodysplasin-A with deletion mutations in collagenous repeats. Hum. Mol. Genet. 7:1661–1669.

Beavis, W. D. 1994. The power and deceit of QTL experiments: lessons from comparative QTL studies. Pp. 250–266 *in* Proceedings of the 49th annual corn and sorghum industry research conference. American Seed Trade Association, Washington, DC.

Bell, M. A., and S. A. Foster. 1994. The evolutionary biology of the threespine stickleback. Oxford Univ. Press, Oxford, U.K.

Bentzen, P., and J. D. McPhail. 1984. Ecology and evolution of sympatric sticklebacks (*Gasterosteus*): specialization for alternative trophic niches in the Enos Lake species pair. Can. J. Zool. 62:2280–2286.

Bentzen, P., M. S. Ridgway, and J. D. McPhail. 1984. Ecology and evolution of sympatric sticklebacks (*Gasterosteus*)—spatial segregation and seasonal habitat shifts in the Enos Lake species pair. Can. J. Zool. 62:2436–2439.

Bergendal, B., J. Klar, C. Stecksen-Blicks, J. Norderyd, and N. Dahl. 2011. Isolated oligodontia associated with mutations in EDARADD, AXIN2, MSX1, and PAX9 genes. Am. J. Med. Genet. Part A 155A:1616–1622.

Bergstrom, C. A. 2002. Fast-start swimming performance and reduction in lateral plate number in threespine stickleback. Can. J. Zool. 80:207–213.

Berner, D. 2011. Size correction in biology: how reliable are approaches based on (common) principal component analysis? Oecologia 166:961–971.

Berner, D., D. C. Adams, A.-C. Grandchamp, and A. P. Hendry. 2008. Natural selection drives patterns of lake-stream divergence in stickleback foraging morphology. J. Evol. Biol. 21:1653–1665.

Berner, D., A.-C. Grandchamp, and A. P. Hendry. 2009. Variable progress toward ecological speciation in parapatry: stickleback across eight lake-stream transitions. Evolution 63:1740–1753.

Berner, D., M. Roesti, A. P. Hendry, and W. Salzburger. 2010a. Constraints on speciation suggested by comparing lake-stream stickleback divergence across two continents. Mol. Ecol. 19:4963–4978.

Berner, D., W. E. Stutz, and D. I. Bolnick. 2010b. Foraging trait (co)variances in stickleback evolve deterministically and do not predict trajectories of adaptive diversification. Evolution 64:2265–2277.

Berner, D., R. Kaeuffer, A.-C. Grandchamp, J. A. M. Raeymaekers, K. Räsänen, and A. P. Hendry. 2011. Quantitative genetic inheritance of morphological divergence in a lake-stream stickleback ecotype pair: implications for reproductive isolation. J. Evol. Biol. 24:1975–1983.

Boden, S. D., Y. S. Liu, G. A. Hair, J. A. Helms, D. Hu, M. Racine, M. S. Nanes, and L. Titus. 1998. LMP-1, a LIM-domain protein, mediates BMP-6 effects on bone formation. Endocrinology 139:5125–5134.

Bolnick, D. I. 2004. Can intraspecific competition drive disruptive selection? An experimental test in natural populations of sticklebacks. Evolution 58:608–618.

Bolnick, D. I., L. K. Snowberg, C. Patenia, W. E. Stutz, T. Ingram, and O. L. Lau. 2009. Phenotype-dependent native habitat preference facilitates divergence between parapatric lake and stream stickleback. Evolution 63:2004–2016.

Broman, K. W., and S. Sen. 2009. A guide to QTL mapping with R/qtl. Springer, New York.

Caldecutt, W. J., and D. C. Adams. 1998. Morphometrics of trophic osteology in the threespine stickleback, *Gasterosteus aculeatus*. Copeia 1998:827–838.

Callahan, N., A. Modesto, R. Meira, F. Seymen, A. Patir, and A. R. Vieira. 2009. Axis inhibition protein 2 (AXIN2) polymorphisms and tooth agenesis. Arch. Oral Biol. 54:45–49.

Chassaing, N., S. Bourthoumieu, M. Cosse, P. Calvas, and M. C. Vincent. 2006. Mutations in EDAR account for one-quarter of non-ED1-related hypohidrotic ectodermal dysplasia. Hum. Mutat. 27:255–259.

Colosimo, P. F., C. L. Peichel, K. Nereng, B. K. Blackman, M. D. Shapiro, D. Schluter, and D. M. Kingsley. 2004. The genetic architecture of parallel armor plate reduction in threespine sticklebacks. PLoS Biol. 2:635–641.

Colosimo, P. F., K. E. Hosemann, S. Balabhadra, G. Villareal Jr., M. Dickson, J. Grimwood, J. Schmutz, R. M. Myers, D. Schluter, and D. M. Kingsley. 2005. Widespread parallel evolution in sticklebacks by repeated fixation of ectodysplasin alleles. Science 307:1928–1933.

Cresko, W. A., A. Amores, C. Wilson, J. Murphy, M. Currey, P. Phillips, M. A. Bell, C. B. Kimmel, and J. H. Postlethwait. 2004. Parallel genetic basis for repeated evolution of armor loss in Alaskan threespine stickleback populations. Proc. Natl. Acad. Sci. USA 101:6050–6055.

Day, T., J. Pritchard, and D. Schluter. 1994. Ecology and genetics of phenotypic plasticity: a comparison of two sticklebacks. Evolution 48:1723–1734.

Deagle, B. E., F. C. Jones, Y. F. Chan, D. M. Absher, D. M. Kingsley, and T. E. Reimchen. 2012. Population genomics of parallel phenotypic evolution in stickleback across stream-lake ecological transitions. Proc. R. Soc. Lond. B 279:1277–1286.

Gerking, S. D. 1994. Feeding ecology of fish. Academic, San Diego, CA.

Giles, N. 1983. The possible role of environmental calcium levels during the evolution of phenotypic diversity in Outer Hebridean populations of the three-spined stickleback, *Gasterosteus aculeatus*. J. Zool. 199:535–544.

Göring, H. H. H., J. D. Terwilliger, and J. Blangero. 2001. Large upward bias in estimation of locus-specific effects from genomewide scans. Am. J. Hum. Genet. 69:1357–1369.

Gross, H. P., and J. M. Anderson. 1984. Geographic variation in the gillrakers and diet of European sticklebacks, *Gasterosteus aculeatus*. Copeia 1984:87–97.

Hagen, D. W., and L. G. Gilbertson. 1972. Geographic variation and environmental selection in *Gasterosteus aculeatus* L. in the pacific northwest, America. Evolution 26:32–51.

Harris, M. P., N. Rohner, H. Schwarz, S. Perathoner, P. Konstantinidis, and C. Nüsslein-Volhard. 2008. Zebrafish *eda* and *edar* mutants reveal conserved and ancestral roles of ectodysplasin signaling in vertebrates. PLoS Genet. 4:e1000206.

Headon, D. J., S. A. Emmal, B. M. Ferguson, A. S. Tucker, M. J. Justice, P. T. Sharpe, J. Zonana, and P. A. Overbeek. 2001. Gene defect in ectodermal

dysplasia implicates a death domain adapter in development. Nature 414:913–916.

Hendry, A. P., and E. B. Taylor. 2004. How much of the variation in adaptive divergence can be explained by gene flow? An evaluation using lake-stream stickleback pairs. Evolution 58:2319–2331.

Henthorn, P. S., M. Raducha, K. N. Fedde, M. A. Lafferty, and M. P. Whyte. 1992. Different missense mutations at the tissue-nonspecific alkaline-phosphatase gene locus in autosomal recessively inherited forms of mild and severe hypophosphatasia. Proc. Natl. Acad. Sci. USA 89:9924–9928.

Heuts, M. J. 1947. Experimental studies on adaptive evolution in *Gasterosteus aculeatus* L. Evolution 1:89–102.

Hoekstra, H. E., and J. A. Coyne. 2007. The locus of evolution: evo devo and the genetics of adaptation. Evolution 61:995–1016.

Hohenlohe, P. A., S. Bassham, P. D. Etter, N. Stiffler, E. A. Johnson, and W. A. Cresko. 2010. Population genomics of parallel adaptation in threespine stickleback using sequenced RAD tags. PLoS Genet. 6:e1000862.

Houston, B., E. Seawright, D. Jefferies, E. Hoogland, D. Lester, C. Whitehead, and C. Farquharson. 1999. Identification and cloning of a novel phosphatase expressed at high levels in differentiating growth plate chondrocytes. Biochim. Biophys. Acta 1448:500–506.

Houston, B., A. J. Stewart, and C. Farquharson. 2004. PHOSPHO1—a novel phosphatase specifically expressed at sites of mineralisation in bone and cartilage. Bone 34:629–637.

Jones, F. C., M. G. Grabherr, Y. F. Chan, P. Russell, E. Mauceli, J. Johnson, R. Swofford, M. Pirun, M. C. Zody, S. White, et al. 2012. The genomic basis of adaptive evolution in threespine sticklebacks. Nature 484:55–61.

Kaeuffer, R., C. Peichel, D. I. Bolnick, and A. P. Hendry. 2012. Convergence and non-convergence in ecological, phenotypic, and genetic divergence across replicate population pairs of lake and stream stickleback. Evolution 66:402–418.

Kahilainen, K., and K. Ostbye. 2006. Morphological differentiation and resource polymorphism in three sympatric whitefish *Coregonus lavaretus* (L.) forms in a subarctic lake. J. Fish Biol. 68:63–79.

Kalamajski, S., A. Aspberg, K. Lindblom, D. Heinegard, and A. Oldberg. 2009. Asporin competes with decorin for collagen binding, binds calcium and promotes osteoblast collagen mineralization. Biochem. J. 423:53–59.

Kere, J., A. K. Srivastava, O. Montonen, J. Zonana, N. Thomas, B. Ferguson, F. Munoz, D. Morgan, A. Clarke, P. Baybayan, et al. 1996. X-linked anhidrotic (hypohidrotic) ectodermal dysplasia is caused by mutation in a novel transmembrane protein. Nat. Genet. 13:409–416.

Kimura, T., M. Shinya, and K. Naruse. 2012. Genetic analysis of vertebral regionalization and number in Medaka (*Oryzias latipes*) inbred lines. G3 2:1317–1323.

Kirsch, T., G. Harrison, E. E. Golub, and H. D. Nah. 2000. The roles of annexins and types II and X collagen in matrix vesicle-mediated mineralization of growth plate cartilage. J. Biol. Chem. 275:35577–35583.

Kitano, J., S. Mori, and C. L. Peichel. 2007. Sexual dimorphism in the external morphology of the threespine stickleback (*Gasterosteus aculeatus*). Copeia 2007:336–349.

Kizawa, H., I. Kou, A. Iida, A. Sudo, Y. Miyamoto, A. Fukuda, A. Mabuchi, A. Kotani, A. Kawakami, S. Yamamoto, et al. 2005. An aspartic acid repeat polymorphism in asporin inhibits chondrogenesis and increases susceptibility to osteoarthritis. Nat. Genet. 37:138–144.

Koyama, K., K. Nakazato, S. K. Min, K. Gushiken, Y. Hatakeda, K. Seo, and K. Hiranuma. 2012. COL11A1 gene is associated with limbus vertebra in gymnasts. Int. J. Sports Med. 33:586–590.

Lammi, L., S. Arte, M. Somer, H. Jarvinen, P. Lahermo, I. Thesleff, S. Pirinen, and P. Nieminen. 2004. Mutations in AXIN2 cause familial tooth agenesis and predispose to colorectal cancer. Am. J. Hum. Genet. 74:1043–1050.

Lande, R., and R. Thompson. 1990. Efficiency of marker-assisted selection in the improvement of quantitative traits. Genetics 124:743–756.

Lavin, P. A., and J. D. McPhail. 1993. Parapatric lake and stream sticklebacks on northern Vancouver Island: disjunct distribution or parallel evolution? Can. J. Zool. 71:11–17.

Lawniczak, M. K. N., S. J. Emrich, A. K. Holloway, A. P. Regier, M. Olson, B. White, S. Redmond, L. Fulton, E. Appelbaum, J. Godfrey, et al. 2010. Widespread divergence between incipient *Anopheles gambiae* species revealed by whole genome sequences. Science 330:512–514.

Leinonen, T., G. Herczeg, J. M. Cano, and J. Merilä. 2011a. Predation-imposed selection on threespine stickleback (*Gasterosteus aculeatus*) morphology: a test of the refuge use hypothesis. Evolution 65:2916–2926.

Leinonen, T., J. M. Cano, and J. Merilä. 2011b. Genetics of body shape and armour variation in threespine sticklebacks. J. Evol. Biol. 24:206–218.

Leinonen, T., R. J. S. McCairns, G. Herczeg, and J. Merilä. 2012. Multiple evolutionary pathways to decreased lateral plate coverage in freshwater threespine sticklebacks. Evolution 66:3866–3875.

Lessells, C. M., and P. T. Boag. 1987. Unrepeatable repeatabilities—a common mistake. Auk 104:116–121.

Li, Y., D. A. Lacerda, M. L. Warman, D. R. Beier, H. Yoshioka, Y. Ninomiya, J. T. Oxford, N. P. Morris, K. Andrikopoulos, F. Ramirez, et al. 1995. A fibrillar collagen gene, COL11A1, is essential for skeletal morphogenesis. Cell 80:423–430.

Liu, Y. H., G. A. Hair, S. D. Boden, M. Viggeswarapu, and L. Titus. 2002. Overexpressed LIM mineralization proteins do not require LIM domains to induce bone. J. Bone Miner. Res. 17:406–414.

Lucek, K., A. Sivasundar, and O. Seehausen. 2012. Evidence of adaptive evolutionary divergence during biological invasion. PLoS One 7:e49377.

Lucek, K., A. Sivasundar, D. Roy, and O. Seehausen. 2013. Repeated and predictable patterns of ecotypic differentiation during a biological invasion: lake-stream divergence in parapatric Swiss stickleback. J. Evol. Biol. 26:2691–2709.

Mackay, T. F. C., E. A. Stone, and J. F. Ayroles. 2009. The genetics of quantitative traits: challenges and prospects. Nat. Rev. Genet. 10:565–577.

Madisen, L., M. Neubauer, G. Plowman, D. Rosen, P. Segarini, J. Dasch, A. Thompson, J. Ziman, H. Bentz, and A. F. Purchio. 1990. Molecular cloning of a novel bone-forming compound—osteoinductive factor. DNA Cell Biol. 9:303–309.

Manly, B. F. J. 2007. Randomization, bootstrap and Monte Carlo methods in biology. Chapman & Hall, Boca Raton, FL.

Mateus, C. S., M. Stange, D. Berner, M. Roesti, B. R. Quintella, M. J. Alves, P. R. Almeida, and W. Salzburger. 2013. Strong genome-wide divergence between sympatric European river and brook lampreys. Curr. Biol. 23:R649–R650.

Matthews, B., K. B. Marchinko, D. I. Bolnick, and A. Mazumder. 2010. Specialization of trophic position and habitat use by sticklebacks in an adaptive radiation. Ecology 91:1025–1034.

McDowall, R. M. 2008. Jordan's and other ecogeographical rules, and the vertebral number in fishes. J. Biogeogr. 35:501–508.

McPhail, J. D. 1984. Ecology and evolution of sympatric sticklebacks (*Gasterosteus*): morphological and genetic evidence for a species pair in Enos Lake, British Columbia. Can. J. Zool. 62:1402–1408.

Mikawa, S., T. Morozumi, S.-I. Shimanuki, T. Hayashi, H. Uenishi, M. Domukai, N. Okumura, and T. Awata. 2007. Fine mapping of a swine quantitative trait locus for number of vertebrae and analysis of an orphan nuclear receptor, germ cell nuclear factor (NR6A1). Genome Res. 17:586–593.

Mikawa, S., S. Sato, M. Nii, T. Morozumi, G. Yoshioka, N. Imaeda, T. Yamaguchi, T. Hayashi, and T. Awata. 2011. Identification of a second gene associated with variation in vertebral number in domestic pigs. BMC Genet. 12:5.

Miller, C. T., D. Yelon, D. Y. R. Stainier, and C. B. Kimmel. 2003. Two *endothelin 1* effectors, *hand2* and *bapx1*, pattern ventral pharyngeal cartilage and the jaw joint. Development 130:1353–1365.

Mitchell-Olds, T., J. H. Willis, and D. B. Goldstein. 2007. Which evolutionary processes influence natural genetic variation for phenotypic traits? Nat. Rev. Genet. 8:845–856.

Monreal, A. W., B. M. Ferguson, D. J. Headon, S. L. Street, P. A. Overbeek, and J. Zonana. 1999. Mutations in the human homologue of mouse dl cause autosomal recessive and dominant hypohidrotic ectodermal dysplasia. Nat. Genet. 22:366–369.

Moodie, G. E. E., and T. E. Reimchen. 1976. Phenetic variation and habitat differences in *Gasterosteus* populations of Queen Charlotte Islands. Syst. Zool. 25:49–61.

Moser, D., M. Roesti, and D. Berner. 2012. Repeated lake-stream divergence in stickleback life history within a Central European lake basin. PLoS One 7:e50620.

Mostowska, A., B. Biedziak, and P. P. Jagodzinski. 2006. Axis inhibition protein 2 (*AXIN2*) polymorphisms may be a risk factor for selective tooth agenesis. J. Hum. Genet. 51:262–266.

Myhre, F., and T. Klepaker. 2009. Body armour and lateral-plate reduction in freshwater three-spined stickleback *Gasterosteus aculeatus*: adaptations to a different buoyancy regime? J. Fish Biol. 75:2062–2074.

Nadeau, N. J., A. Whibley, R. T. Jones, J. W. Davey, K. K. Dasmahapatra, S. W. Baxter, M. A. Quail, M. Joron, R. H. Ffrench-Constant, M. L. Blaxter, et al. 2012. Genomic islands of divergence in hybridizing *Heliconius* butterflies identified by large-scale targeted sequencing. Philos. Trans. R. Soc. Lond. B 367:343–353.

Nei, M., and F. Tajima. 1981. DNA polymorphism detectable by restriction endonucleases. Genetics 97:145–163.

Nichols, K. M., P. A. Wheeler, and G. H. Thorgaard. 2004. Quantitative trait loci analyses for meristic traits in *Oncorhynchus mykiss*. Environ. Biol. Fish. 69:317–331.

Nielsen, R. 2005. Molecular signatures of natural selection. Annu. Rev. Genet. 39:197–218.

Oleksyk, T. K., M. W. Smith, and S. J. O'Brien. 2010. Genome-wide scans for footprints of natural selection. Philos. Trans. R. Soc. Lond. B 365:185–205.

Orr, H. A. 1998. The population genetics of adaptation: the distribution of factors fixed during adaptive evolution. Evolution 52:935–949.

Pfaender, J., F. W. Miesen, R. K. Hadiaty, and F. Herder. 2011. Adaptive speciation and sexual dimorphism contribute to diversity in form and function in the adaptive radiation of Lake Matano's sympatric roundfin sailfin silversides. J. Evol. Biol. 24:2329–2345.

Phillips, P. C. 2005. Testing hypotheses regarding the genetics of adaptation. Genetica 123:15–24.

R Development Core Team 2013. R: a language and environment for statistical computing. R Foundation for Statistical Computing, Austria, Vienna.

Ravinet, M., P. A. Prodoehl, and C. Harrod. 2013. Parallel and nonparallel ecological, morphological and genetic divergence in lake-stream stickleback from a single catchment. J. Evol. Biol. 26:186–204.

Reimchen, T. E. 1994. Predators and morphological evolution in threespine stickleback. Pp. 240–273 *in* M. A. Bell and S. A. Foster, eds. The evolutionary biology of the threespine stickleback. Oxford Univ. Press, Oxford, U.K.

Reimchen, T. E., E. M. Stinson, and J. S. Nelson. 1985. Multivariate differentiation of parapatric and allopatric populations of threespine stickleback in the Sangan River watershed, Queen Charlotte Islands. Can. J. Zool. 63:2944–2951.

Reist, J. D. 1985. An empirical evaluation of several univariate methods that adjust for size variation in morphometric data. Can. J. Zool. 63:1429–1439.

Ren, D. R., J. Ren, G. F. Ruan, Y. M. Guo, L. H. Wu, G. C. Yang, L. H. Zhou, L. Li, Z. Y. Zhang, and L. S. Huang. 2012. Mapping and fine mapping of quantitative trait loci for the number of vertebrae in a White Duroc x Chinese Erhualian intercross resource population. Anim. Genet. 43:545–551.

Roberts, S., S. Narisawa, D. Harmey, J. L. Millan, and C. Farquharson. 2007. Functional involvement of PHOSPHO1 in matrix vesicle-mediated skeletal mineralization. J. Bone Miner. Res. 22:617–627.

Rockman, M. V. 2011. The QTN program and the alleles that matter for evolution: all that's gold does not glitter. Evolution 66:1–17.

Roesti, M., A. P. Hendry, W. Salzburger, and D. Berner. 2012a. Genome divergence during evolutionary diversification as revealed in replicate lake-stream stickleback population pairs. Mol. Ecol. 21:2852–2862.

Roesti, M., W. Salzburger, and D. Berner. 2012b. Uninformative polymorphisms bias genome scans for signatures of selection. BMC Evol. Biol. 12:94.

Roesti, M., D. Moser, and D. Berner. 2013. Recombination in the threespine stickleback genome—patterns and consequences. Mol. Ecol. 22:3014–3027.

Roesti, M., S. Gavrilets, A. P. Hendry, W. Salzburger, and D. Berner. 2014. The genomic signature of parallel adaptation from shared genetic variation. Mol. Ecol. *In press*.

Rohlf, F. J. 2001. tpsDig, tpsRelw, tpsRegr. Distributed by the author. Department of Ecology and Evolution, State University of New York, Stony Brook, NY.

Sanderson, S. L., A. Y. Cheer, J. S. Goodrich, J. D. Graziano, and W. T. Callan. 2001. Crossflow filtration in suspension-feeding fishes. Nature 412:439–441.

Schluter, D., and J. D. McPhail. 1992. Ecological character displacement and speciation in sticklebacks. Am. Nat. 140:85–108.

Sharpe, D. M. T., K. Räsänen, D. Berner, and A. P. Hendry. 2008. Genetic and environmental contributions to the morphology of lake and stream stickleback: implications for gene flow and reproductive isolation. Evol. Ecol. Res. 10:849–866.

Song, Y.-Q., K. M. C. Cheung, D. W. H. Ho, S. C. S. Poon, K. Chiba, Y. Kawaguchi, Y. Hirose, M. Alini, S. Grad, A. F. Y. Yee, et al. 2008. Association of the asporin D14 allele with lumbar-disc degeneration in Asians. Am. J. Hum. Genet. 82:744–747.

Stern, D. L., and V. Orgogozo. 2008. The loci of evolution: how predictable is genetic evolution? Evolution 62:2155–2177.

Stinchcombe, J. R., and H. E. Hoekstra. 2008. Combining population genomics and quantitative genetics: finding the genes underlying ecologically important traits. Heredity 100:158–170.

Stölting, K. N., R. Nipper, D. Lindtke, C. Caseys, S. Waeber, S. Castiglione, and C. Lexer. 2013. Genomic scan for single nucleotide polymorphisms reveals patterns of divergence and gene flow between ecologically divergent species. Mol. Ecol. 22:842–855.

Storz, J. F. 2005. Using genome scans of DNA polymorphism to infer adaptive population divergence. Mol. Ecol. 14:671–688.

Storz, J. F., and C. W. Wheat. 2010. Integrating evolutionary and functional approaches to infer adaptation at specific loci. Evolution 64:2489–2509.

Swain, D. P. 1992. The functional basis of natural selection for vertebral traits of larvae in the stickleback *Gasterosteus aculeatus*. Evolution 46:987–997.

The UniProt Consortium. 2013. Update on activities at the Universal Protein Resource (UniProt) in 2013. Nucleic Acids Res. 41:D43–D47.

Thompson, C. E., E. B. Taylor, and J. D. McPhail. 1997. Parallel evolution of lake-stream pairs of threespine sticklebacks (*Gasterosteus*) inferred from mitochondrial DNA variation. Evolution 51:1955–1965.

Thouverey, C., A. Strzelecka-Kiliszek, M. Balcerzak, R. Buchet, and S. Pikula. 2009. Matrix vesicles originate from apical membrane microvilli of mineralizing osteoblast-like saos-2 cells. J. Cell. Biochem. 106:127–138.

Tompson, S. W., C. A. Bacino, N. P. Safina, M. B. Bober, V. K. Proud, T. Funari, M. F. Wangler, L. Nevarez, L. Ala-Kokko, W. R. Wilcox, et al. 2010. Fibrochondrogenesis results from mutations in the COL11A1 type XI collagen gene. Am. J. Hum. Genet. 87:708–712.

Van Wesenbeeck, L., P. R. Odgren, F. P. Coxon, A. Frattini, P. Moens, B. Perdu, C. A. MacKay, E. Van Hul, J.-P. Timmermans, F. Vanhoenacker, et al. 2007. Involvement of PLEKHM1 in osteoclastic vesicular transport and osteopetrosis in incisors absent rats and humans. J. Clin. Invest. 117:919–930.

Voight, B. F., S. Kudaravalli, X. Wen, and J. K. Pritchard. 2006. A map of recent positive selection in the human genome. PLoS Biol. 4:e72.

Wake, D. B., M. H. Wake, and C. D. Specht. 2011. Homoplasy: from detecting pattern to determining process and mechanism of evolution. Science 331:1032–1035.

Wang, W., and T. Kirsch. 2002. Retinoic acid stimulates annexin-mediated growth plate chondrocyte mineralization. J. Cell Biol. 157:1061–1069.

Ward, A. B., and E. L. Brainerd. 2007. Evolution of axial patterning in elongate fishes. Biol. J. Linn. Soc. 90:97–116.

Weiss, M. J., D. E. C. Cole, K. Ray, M. P. Whyte, M. A. Lafferty, R. A. Mulivor, and H. Harris. 1988. A missense mutation in the human liver/bone/kidney alkaline-phosphatase gene causing a lethal form of hypophosphatasia. Proc. Natl. Acad. Sci. USA 85:7666–7669.

Wray, G. A. 2007. The evolutionary significance of cis-regulatory mutations. Nat. Rev. Genet. 8:206–216.

Wund, M. A., J. A. Baker, B. Clancy, J. L. Golub, and S. A. Foster. 2008. A test of the "Flexible stem" model of evolution: ancestral plasticity, genetic accommodation, and morphological divergence in the threespine stickleback radiation. Am. Nat. 172:449–462.

Xu, S. Z. 2003. Theoretical basis of the Beavis effect. Genetics 165:2259–2268.

Yeaman, S., and M. C. Whitlock. 2011. The genetic architecture of adaptation under migration-selection balance. Evolution 65:1897–1911.

Associate Editor: C. Sgro

Supporting Information

Additional Supporting Information may be found in the online version of this article at the publisher's website:

Figure S1. Genome-wide LOD profiles for all eight traits.

Figure S2. Body size (quantified as geometric morphometric centroid size, in millimeters) in relation to vertebral number.

Table S1. Characterization of additional, suggestive ($0.05 \leq P < 0.1$) QTLs for skeletal divergence between lake and stream stickleback.